Stratospheric ozone observations inconsistent with high solar cycle spectral variations

Ball, W.T.[1], Haigh, J.D.[2], Rozanov, E.V.[1,3], Kuchar, A.[3,4], Sukhodolov, T.[1,3], Tummon, F.[3], Shapiro, A.V.[1] & Schmutz, W.[1]

[1]*Physikalisch-Meteorologisches Observatorium Davos World Radiation Centre, Dorfstrasse 33, 7260 Davos Dorf, Switzerland*

[2]*Grantham Institute - Climate Change and the Environment, Imperial College London, South Kensington Campus, London SW7 2AZ, UK*

[3]*Institute for Atmospheric and Climate Science, Swiss Federal Institute of Technology Zurich, Universitaetstrasse 16, CHN, CH-8092 Zurich, Switzerland*

[4]*Department of Atmospheric Physics, Faculty of Mathematics and Physics, Charles University in Prague, V Holesovickach 2, 180 00 Prague 8, Czech Republic*

Solar variability can influence surface climate, for example by affecting the mid-to-high latitude surface pressure gradient associated with the North Atlantic Oscillation [1]. One key mechanism behind such an influence is the absorption of solar ultraviolet (UV) radiation by ozone in the tropical stratosphere, a process that modifies temperature and wind patterns and hence wave propagation and atmospheric circulation [2–5]. The amplitude of UV variability is uncertain, yet it directly affects the magnitude of the climate response [6]: observations from the SOlar Radiation and Climate Experiment (SORCE) satellite [7] show broadband changes up to three-times larger than previous measurements [8,9]. Here we present estimates of the

stratospheric ozone variability during the solar cycle. Specifically, we estimate the photolytic response of stratospheric ozone to changes in spectral solar irradiance by calculating the difference between a reference chemistry-climate model simulation of ozone variability driven only by transport (with no changes in solar irradiance) and observations of ozone concentrations. Subtracting the reference from simulations with time-varying irradiance, we can evaluate different datasets of measured and modelled spectral irradiance. We find that at altitudes above pressure levels of 5 hPa, the ozone response to solar variability simulated using the SORCE spectral solar irradiance data are inconsistent with the observations.

Solar UV radiation at wavelengths shorter than 242 nm leads to the creation of ozone in the middle atmosphere, while longer wavelength UV initiates its destruction (Fig. 1). It follows that the ozone distribution is sensitive to spectral solar irradiance (SSI) and, conversely, that observed changes in ozone can reveal information on SSI variations [8–10]. This is especially true in the tropical upper stratosphere where photochemical processes dominate over transport.

Continuous satellite measurements of the solar UV spectrum have been acquired since 1978. Two instruments on the SORCE satellite, the SOLar STellar Irradiance Comparison Experiment (SOLSTICE) [11] and the Spectral Irradiance Monitor (SIM) [12], have been monitoring UV irradiance since 2003. Early versions of SORCE data showed very large solar cycle variations (up to 10 times larger at some wavelengths) compared to models [13,14]. These models show good agreement with earlier observations from the Upper Atmosphere Research Satellite (UARS) Solar Ultraviolet Spectral Irradiance Monitor (SUSIM) instrument operating between 1991 and 2005 [8]. The larger solar cycle changes in SORCE are probably due to insufficient correction of sensor degradation and drifts [10,13,14]. The magnitude of solar cycle variations have reduced in recent releases, but significant uncertainties remain regarding the true variation (see, e.g., Fig. 3 of ref [[8]] and Fig. 4 of ref [[[9]]).

The total solar irradiance (TSI) amplitude of the current solar cycle (which began in December 2008) is ∼65% of the previous cycle (1996–2008), and TSI has decreased between recent solar minima by 36% [15]. Another measure of solar activity, the open solar flux [16], which is the solar flux that escapes into the solar system and is related to the solar surface magnetic flux that drives irradiance changes, has decreased by ∼59% over the same period following a century in a grand maximum state [17]. It has been suggested [18] that the larger SORCE UV solar cycle changes indicate that the Sun's spectral variability may have behaved differently during the last solar cycle. The magnitude of both TSI, on all timescales, and the 27-day solar rotational variability at UV, visible and infra-red wavelengths, is well quantified by observations and reproduced by models. Sunspots and faculae drive irradiance variations on daily to centennial timescales, and a change in the solar cycle variability, following SORCE observations, would require their intrinsic wavelength dependent intensities to change. However, variability on rotational timescales at all wavelengths and the well-quantified solar cycle TSI changes would have to be conserved. This is highly unlikely, but does not preclude the possibility that the SORCE magnitude is correct.

To investigate SORCE solar cycle spectral changes over more than half a solar cycle, we extrapolate SORCE back to 1974 using the SATIRE-S [19] solar irradiance model (see methods), with two essential requirements: (i) that the integrated spectral irradiance, the TSI, is in good agreement with the PMOD composite of TSI observations, and (ii) that the UV solar cycle changes of SORCE are conserved (see Methods). Figure 2a shows SATIRE-S, NRLSSI (or 'Lean' model, see methods) and extrapolated SORCE ('eSORCE') from 1991 to 2012 integrated over 250–300 nm. Interestingly, from 2009 SORCE/SIM UV agrees well with SATIRE-S. We summarise the impact of the different SSI from SATIRE-S and SORCE on the solar cycle ozone response in Fig 1.

The solar cycle ozone response is usually extracted from ozone observations using multi-linear regression (MLR; see Methods). However, results have varied widely. Early analyses generally showed a positive correlation throughout the middle atmosphere, with a peak amplitude of $\sim$2% at 40 km ($\sim$5 hPa) [20]. Some recent studies have suggested a negative relationship at around 50 km in the lower mesosphere (e.g. around -1.2% [21], -1.5% [22], -0.5% [9]) while others have not ($>$+1% [23]). Atmospheric models have shown that the negative signal is consistent with the larger UV variations from earlier versions of SORCE data, although the predicted magnitude reduces with updated versions (e.g. from -1.6% with SOLSTICE version 10 to -0.2% with version 12 [8]).

Uncertainties associated with both MLR analyses (e.g. the possibility of aliasing between input proxies [24]) and model simulations (e.g. their representation of transport processes and how these respond to the Sun) mean that it has not been possible to narrow the uncertainty range of SSI variations. To circumvent these issues we calculate ozone changes between 1991 and 2012 using the full photochemical capabilities of the SOlar Climate Ozone Links (SOCOL; see methods) chemistry-climate model (CCM) forced by nudged dynamical fields from ERA-Interim reanalysis data (see methods). We note that the uncertainties in the applied meteorological fields can lead to inaccuracy in the ozone trend definition. For example, ERA-Interim, applied here, is known to have an unrealistic negative trend in annual mean residual upwelling averaged over 30°S–30°N [25], though ref [[25]] focused on altitudes below 10 hPa ($\sim$32 km), and ERA-Interim confined to the equatorial region is similar to MERRA and JRA-55 reanalyses. This difference relates mostly to the shallow branch of the Brewer-Dobson Circulation, while the upper branch is well reproduced. An increase in lower stratosphere tropical upwelling by $\sim$100% strongly affects ozone below 20 hPa ($\sim$27 km), though only by about 2% above this level [26]. We estimate that even a 5% error in the lower stratosphere tropical upwelling should not lead to a visible impact above 10 hPa, which is the focus of this study.

We perform three simulations, the first using a solar-minimum constant-Sun. Zonal-mean tropical ozone at 1.6 hPa from that simulation is shown by the red curve in Fig. 2b and compared with the Stratospheric Water and OzOne Satellite Homogenized (SWOOSH) ozone observational dataset [27] in black. The model reproduces well the overall magnitude of the semi-annual variation and inter-annual variability shown by the measurements. The difference between the two curves, shown in Fig. 2c by the grey curve (with a 24-month running mean in black and shaded 1σ uncertainty range), clearly indicates a solar cycle signal in the observed data.

The other two model simulations use varying SSI from the SATIRE-S model and from eS-ORCE, as exemplified in Fig. 2a. Differences between these simulations and the constant-Sun run are shown in Fig. 2c by the blue and green curves respectively. Both show a solar cycle influence, although SATIRE-S is of smaller magnitude than SWOOSH and eSORCE is inverted at this altitude, consistent with the larger UV variations.

We perform MLR (see Methods) throughout the 30–0.25 hPa tropical region; the nudged simulations provide a clean output, free of model internal variability, eliminating the need for ensemble simulations to detect the solar signal. We perform the same analysis on the SWOOSH and the Global OZone Chemistry And Related Datasets for the Stratosphere (GOZCARDS) [28] ozone datasets. Fig. 3 shows that the simulation using SATIRE-S is more like the results from the measured data than that using eSORCE.

To further test the robustness of these results we compare the linear photolytic trends between solar minimum and solar maximum over two solar maximum-to-minimum periods: 1991/07–1996/05 and 2002/02–2008/12. We remove the dynamical response by subtracting the constant-Sun simulation from the other simulations and observed merged ozone datasets (as in Fig. 2c), leaving a residual photolytic response. Additionally, we include data from SBUV-Merged and SBUV-Mod [29] ozone datasets in the latter period, but not prior to 2002 due to steps in the data where there is a change in the underlying instrument data used; SWOOSH has too many data gaps to consider the 1996–2002 period (see Fig. 2c).

We calculate the linear trends and uncertainties from the residuals (see methods). The results are shown in Fig. 4. Caution is needed for results above 1 hPa; the large diurnal cycle in ozone (up to 10% [28]) means that observations from different times of the day need to be adjusted to ensure this is taken into account: SWOOSH does not extend beyond 1 hPa, the GOZCARDS authors advise caution [28]; and the SBUV merged datasets do not correct for it [27].

The residuals of all four ozone datasets show broadly the same solar cycle ozone response, peaking at ∼4 hPa; the SBUV responses are slightly smaller than GOZCARDS and SWOOSH above 10 hPa and are not significantly different from zero above 2 hPa. GOZCARDS and SWOOSH agree with each other in both time periods, except at 4 hPa where the earlier period has a larger response; the 1991–1996 UV change was larger than for 2002–2008 and may explain some of this difference. The fact that the solar cycle ozone responses are similar in both solar cycles indicates that the intrinsic properties of features driving solar cycle UV changes remained similar in both periods and it is, therefore, unlikely that the behaviour of the Sun's spectral variability changed significantly between cycles.

Fig. 4 also shows SORCE and SATIRE-S simulation results as green and blue shading, respectively (shading encompasses the linear trend fitting and errors of both periods, which have similar magnitudes). The actual solar cycle response, calculated by taking the difference of six-month means at solar maximum and solar minimum, agree within the uncertainty of the trend fitting, showing that linear fitting is appropriate. The red shading represents NRLSSI for 2002–2008 only. The merged ozone dataset residuals, for both periods, reveal statistically significant results that do not agree with the simulation using SORCE above ∼5 hPa and, rather, have similar ozone profiles to those using SATIRE-S and NRLSSI.

The simulation profile shapes in Fig. 4 differ from Fig. 3 because the dynamical solar response is included; the lower altitude positive response and negative response higher up are indicative of a slowing of the Brewer-Dobson circulation in agreement with theory [3]. Subtracting the constant-Sun (not shown) from the SATIRE-S and SORCE profiles give photolytic responses similar in shape and magnitude to those in Fig. 4.

Overall, we find that the ozone observations are not consistent with SORCE UV solar cycle changes. Our novel analysis provides a unique assessment of spectral solar cycle changes and strongly supports suggestions [10,13,14] that SORCE solar cycle trends at longer UV wavelengths, using SIM above 247 nm, are unlikely to be correct. Our study also shows that SATIRE-S spectral changes, which are similar to older observations from UARS/SUSIM, produce ozone changes more consistent with observations.

Solar UV variability influences the climate near Earth's surface through heating the middle atmosphere and subsequent dynamical coupling between the stratosphere and troposphere. Details of the changes in the UV spectrum are crucial to the mechanisms involved and to the resulting impacts. A recent study [30], concerned with the potential for declining solar activity to mitigate global warming, has shown that the effect on near-surface temperature in the North Atlantic depends sensitively on the choice of UV spectrum and our work suggests that the effect is probably at the lower end of those considered in that study. If climate models are not able to reproduce the observed signals at the surface using the weaker UV changes it may be that they are missing some necessary mechanism(s). A better knowledge of SSI variability is essential to advance our understanding of how the Sun influences surface climate and might do so in future.

Methods

SSI datasets. : Four SSI datasets were used: constant-Sun using the mean of 2008/11–2009/01 from SATIRE-S; SATIRE-S model; NRLSSI model; extrapolated-SORCE. Each dataset was bias corrected to give the same absolute fluxes as SATIRE-S at the solar minimum in 2008.

SATIRE-S and NRLSSI solar models. SATIRE-S is a semi-empirical solar model [19] constructed using time-independent model intensities of sunspots, faculae and the quiet-Sun. SATIRE-S agrees with TSI observations better than any other TSI model, reproduces rotational variability well and shows good agreement with UARS/SUSIM [31] solar cycle variability below 400 nm [8,32]. The Naval Research Laboratory Spectral Solar Irradiance ('NRLSSI' or 'Lean') model [33], has previously been the standard solar irradiance input in climate studies. NRLSSI is an empirical model constructed by regressing the rotational variability from UARS/SOLSTICE observations with indices for facular and sunspot contributions and scaling this to the solar cycle variability (coefficients of variability for wavelengths longer than 400 nm are calculated using model atmospheres regressed with the indices and scaled so the full integral gives the correct TSI). Compared to SATIRE-S, NRLSSI displays slightly lower solar cycle UV variability than SATIRE-S above 250 nm [8,32] (see Fig. 2a). SATIRE-S and NRLSSI cover wavelengths from the 115 to 160 000 and 120 to 100 000 nm, respectively.

SORCE data. We use SORCE data from SOLSTICE v13 below 247 nm and SIM v20 between 310 and 1598 nm; the changeover at 247 nm was chosen due to higher correlations of SORCE/SIM with SATIRE-S at and above this wavelength (see below). We note that the more recent releases, SIM v22 and SOLSTICE v14, show nearly identical UV solar cycle trends for the 2004-2008 extrapolation period. Newer versions of SIM and SOLSTICE show substantial differences with respect to earlier versions [34]

Extrapolated-SORCE (eSORCE) solar irradiance data. To construct the extrapolated-SORCE (eSORCE) from the SORCE observational record (2003-present), a stable period is needed to regress against and make a reliable extrapolation. Unfortunately, SORCE is not stable at all times with respect to proxies, e.g. F10.7 cm radio flux, Mg II index, and models. Here, we use SATIRE-S as the basis for extrapolation because it shows very good agreement in the UV with the aforementioned proxies [8,9].

Our aim is to reconstruct SORCE-like solar cycle, multi-year spectral variations. The spectral, 27-day, rotational variability is in good agreement with the SATIRE-S model at almost all wavelengths [13], but this short-term variability can interfere in the calculation of regression coefficients. Therefore, we regress only the smoothed time series of SORCE with SATIRE-S for the extrapolation, and add the rotational variability of SATIRE-S onto the extrapolated product. We detrend SIM version 20 and SOLSTICE version 13 data at each wavelength by smoothing with a gaussian kernel with a 1σ window of 135 days (i.e. 5-solar rotations).

In Supplementary Figure 1, we show four examples of smoothed SORCE time series plotted (left axes) against SATIRE-S for (a) SOLSTICE (blue colours) at 176 nm, (b) SOLSTICE and SIM (red/orange colours) at 247 nm, (c) SIM at 311 nm and (d) SIM at 499 nm, relative to the mean value of the time series. Light colours represent times prior to 2004/09/01, medium colours between 2004/09/01 and 2008/08/31, and dark after 2008/08/31. In black, the F10.7 cm radio flux is plotted (right axes) against SATIRE-S (dotted, solid and dashed for the same three time periods, respectively). The steps in gradient are clear after 2008/08/31. The difference in gradient prior to 2004/09/01 is clearer only in comparison to SIM. In contrast, SATIRE-S shows similar behavior to the F10.7 cm radio flux at all wavelengths, i.e. returning to similar activity levels after 2008 as before (although at 499 nm the scatter at maximum is larger, as should be expected at non-UV wavelengths). Therefore, the change in gradient between cycles is a part of SORCE and makes extrapolation of the full time series problematic.

We note that the gradient prior to 2004/09/01 is larger in SIM than for the period from 2004 to 2008. If the gradient from the whole period prior to 2008 were used, this would enhance ozone destruction and lead to a more negative ozone response in the upper stratosphere (see Figures 1 and 4). It is appropriate to use the 2004–2008 period for extrapolation for several reasons: the period is relatively stable, using this period leads to a more conservative estimate of the upper stratospheric ozone response (i.e., less negative), and this is approximately the period used for studies into the impact of SORCE-like UV solar cycle changes [6,21,22,30].

Combining SOLSTICE and SIM data can only be done above 240 nm, from where SIM is available. The uncertainty in the SOLSTICE long-term trend above 285 nm is larger than the solar cycle variation [8]. There is currently no consensus among the SORCE instrument scientists on where to make the transition from SOLSTICE to SIM in wavelength (personal communication, Marty Snow), so based on agreement with respect to SATIRE-S, since the correlation coefficient with respect to SIM exceeds SOLSTICE here, we choose the changeover wavelength at 247 nm. In addition, we note that earlier studies, investigating the impact of SORCE fluxes on the atmosphere, applied SIM from 200 nm [6,10,21,30] and 240 nm [10,21,22], so our choice is consistent with these studies. We extrapolate all wavelengths from 115 to 310 nm, using the regression coefficients calculated with respect to SATIRE-S, to the period 1974–2014. In Supplementary Figure 2, we show the percentage change between three-month averages centred on 2004/09/01 and 2008/08/31 from the original (SOLSTICE, black; SIM, grey) and extrapolated-SORCE (green) datasets and SATIRE-S (blue). While the extrapolation is not perfect in reproducing the variability at every wavelength, the general spectral behavior is in good agreement, as exemplified by the horizontal lines which represent the integrated flux change for SOLSTICE (black, dashed) and eSORCE (green, solid) for 176–242 nm, and for SIM (grey, dashed) and eSORCE for 247–310 nm.

Above 1598 nm, SIM time series show large jumps and monotonic trends for the whole period, though the absolute change is small. Since the integrated flux in SIM above 1598 nm shows very little variability relative to TSI [13], it is reasonable to use SATIRE-S for these wavelengths, which also shows little variability. For the 310–1598 nm region, we regress SIM to SATIRE-S as for the UV wavelengths.

At this stage, there is full coverage from 115 to 160,000 nm. However, the change in total solar irradiance from the spectral integral does not agree with the PMOD TSI composite. This is because the large inverse visible and infrared trends overcompensate for the large UV trends. Since we need to achieve good agreement with the PMOD composite of TSI, and maintain the SORCE UV variability, we decrease the cycle trends in the 310–1598 nm range with a single factor of 0.15, determined by minimising the difference with respect to the PMOD TSI composite.

Now, the integral is in reasonable agreement with the PMOD composite at all times, as seen in the smoothed time series in the bottom panel of Supplementary Figure 3. Here, 'SORCE' is the integral of SOLSTICE below 247 nm, SIM from 247 to 1598 nm, and SATIRE-S above.

The final step is to add the rotational variability of SATIRE-S, originally removed by the smoothing applied earlier. This completes the eSORCE dataset. Supplementary Figure 3 shows, from top to bottom, eSORCE (green) for 176–242 nm, 250–300 nm, 400–700 nm and TSI (smoothed only) for the full period, compared to SATIRE-S (blue) and the original SORCE data (black, smoothed; grey, daily). It is clear that the extrapolation is consistent and in good agreement with SORCE during the overlap period (except for the magnitude of change in the 400–700 nm band, and TSI, which now agrees well with the PMOD TSI Composite). eSORCE, therefore, provides a consistent dataset that gives a good estimate of SORCE-like variability for three full solar cycles that can be useful to investigate the impact of SORCE-like irradiance changes on a climate relevant timescale.

Ozone Data. A summary of the ozone merged datasets, and an intercomparison, are given by ref [[27]]. These data are monthly, zonally averaged, homogenised, and bias-corrected ozone datasets spanning 1984–2013, typically covering latitudes between 48 S and 48 N. All datasets were interpolated onto the SOCOL model pressure levels. Data were then bias corrected to the constant-Sun simulation mean values for the six-month average centred on the December 2008 solar minimum.

Nudged Chemistry Climate Model. SOCOL uses the ECHAM-5 atmospheric general circulation model with a resolved stratosphere and online coupled chemistry module (MEZON) [35]. We use the Stratospheric Processes and their Role in Climate (SPARC) International Global Atmospheric Chemistry (IGAC) Chemistry Climate Model Initiative (CCMI) [36] boundary conditions and external forcings (except for the Sun). We nudge the vorticity and divergence of the wind fields, temperature, and surface level pressure with ERA-Interim [37] between 1983 and 2012, only considering data from 1991 to 2012; 1983–1990 are considered as model spin-up years. A run was also performed using the NRLSSI model for 2002–2010; spin-up was for 1994–2001.

Trend analysis. We perform linear trend analysis using the non-parametric Theil-Sen trend estimation, which is more accurate than a standard linear regression for non-gaussian data.

Multi-linear regression. We have applied Multiple Linear Regression (MLR) similar to ref[[38]] using the 10.7 cm radio flux as a solar proxy, stratospheric aerosol optical depth (SAOD) for volcanic eruptions [39], an ENSO index [40] representing El Niño Southern Oscillation variability, and two modes of the Quasi-Biennial Oscillation (QBO; extracted by principal component analysis (PCA) from the residuals of our regression model excluding QBO regressors and AR2 zonal mean zonal winds between ±10°N and 10 to 50 hPa) and the Equivalent Effective Stratospheric Chlorine (EESC) for chlorine loading. To avoid the auto-correlation of residuals we use an iterative algorithm to model residuals as a second-order auto-regressive process (AR2). Statistical significance of the regression coefficients was evaluated with a t-test. We found similar results using a more robust ‘bias-corrected and accelerated’ (BCA) bootstrap percentile method [41] based on 10000 samples, which does not assume the data distribution *a priori*.

Code availability The SOCOL model code is available on request.

Data availability. The eSORCE dataset is available on request.

1. Gray, L. J. *et al.* A lagged response to the 11 year solar cycle in observed winter atlantic/european weather patterns. *Journal of Geophysical Research-Atmospheres* **118**, 13405–13420 (2013).
2. Haigh, J. The impact of solar variability on climate. *Science* **272**, 981–984 (1996).
3. Kodera, K. & Kuroda, Y. Dynamical response to the solar cycle. *Journal of Geophysical Research (Atmospheres)* **107**, 4749 (2002).
4. Simpson, I. R. & Blackburn, J. D., M. & Haigh. The role of eddies in driving the tropospheric response to stratospheric heating perturbations. *Journal of the Atmospheric Sciences* **66**, 1347–1365 (2009).
5. Gray, L. J. *et al.* Solar Influences on Climate. *Reviews of Geophysics* **48**, 4001 (2010).
6. Ineson, S. *et al.* Solar forcing of winter climate variability in the Northern Hemisphere. *Nature Geoscience* **4**, 753–757 (2011).
7. Rottman, G. The SORCE Mission. *Solar Physics* **230**, 7–25 (2005).
8. Ball, W. T., Krivova, N. A., Unruh, Y. C., Haigh, J. D. & Solanki, S. K. A New SATIRE-S Spectral Solar Irradiance Reconstruction for Solar Cycles 21-23 and Its Implications for Stratospheric Ozone*. *Journal of Atmospheric Sciences* **71**, 4086–4101 (2014). `1408.0365`.

9. Ball, W. T., Mortlock, D. J., Egerton, J. S. & Haigh, J. D. Assessing the relationship between spectral solar irradiance and stratospheric ozone using Bayesian inference. *Journal of Space Weather and Space Climate* **4**, A25 (2014). `1408.3559`.

10. Ermolli, I. *et al.* Recent variability of the solar spectral irradiance and its impact on climate modelling. *Atmospheric Chemistry and Physics* **13**, 3945–3977 (2013). `1303.5577`.

11. McClintock, W. E., Rottman, G. J. & Woods, T. N. Solar-Stellar Irradiance Comparison Experiment II (Solstice II): Instrument Concept and Design. *Solar Physics* **230**, 225–258 (2005).

12. Harder, J. W., Fontenla, J. M., Pilewskie, P., Richard, E. C. & Woods, T. N. Trends in solar spectral irradiance variability in the visible and infrared. *Geophysical Research Letters* **36**, 7801 (2009).

13. Ball, W. T., Unruh, Y. C., Krivova, N. A., Solanki, S. & Harder, J. W. Solar irradiance variability: A six-year comparison between SORCE observations and the SATIRE model. *Astronomy & Astrophysics* **530**, A71 (2011).

14. Lean, J. L. *et al.* How Does the Sun's Spectrum Vary? *Journal of Climate* **25**, 2555–2560 (2012).

15. Fröhlich, C. Evidence of a long-term trend in total solar irradiance. *Astronomy & Astrophysics* **501**, L27–L30 (2009).

16. Lockwood, M. Reconstruction and Prediction of Variations in the Open Solar Magnetic Flux and Interplanetary Conditions. *Living Reviews in Solar Physics* **10**, 4 (2013).

17. Usoskin, I. G., Solanki, S. K. & Kovaltsov, G. A. Grand minima of solar activity during the last millennia. In Mandrini, C. H. & Webb, D. F. (eds.) *IAU Symposium*, vol. 286 of *IAU Symposium*, 372–382 (2012).

18. Fontenla, J. M., Curdt, W., Haberreiter, M., Harder, J. & Tian, H. Semiempirical Models of the Solar Atmosphere. III. Set of Non-LTE Models for Far-Ultraviolet/Extreme-Ultraviolet Irradiance Computation. *The Astrophysical Journal* **707**, 482–502 (2009).

19. Yeo, K. L., Krivova, N. A., Solanki, S. K. & Glassmeier, K. H. Reconstruction of total and spectral solar irradiance from 1974 to 2013 based on KPVT, SoHO/MDI, and SDO/HMI observations. *Astronomy & Astrophysics* **570**, A85 (2014). `1408.1229`.

20. Austin, J. *et al.* Coupled chemistry climate model simulations of the solar cycle in ozone and temperature. *Journal of Geophysical Research (Atmospheres)* **113**, 11306 (2008).

21. Haigh, J. D., Winning, A. R., Toumi, R. & Harder, J. W. An influence of solar spectral variations on radiative forcing of climate. *Nature* **467**, 696–699 (2010).

22. Merkel, A. W. *et al.* The impact of solar spectral irradiance variability on middle atmospheric ozone. *Geophysical Research Letters* **38**, 13802 (2011).

23. Hood, L. L. *et al.* Solar signals in cmip-5 simulations: the ozone response. *Quarterly Journal of the Royal Meteorological Society* (2015).

24. Chiodo, G., Marsh, D. R., Garcia-Herrera, R., Calvo, N. & García, J. A. On the detection of the solar signal in the tropical stratosphere. *Atmospheric Chemistry & Physics* **14**, 5251–5269 (2014).

25. Abalos, M., Legras, B., Ploeger, F. & Randel, W. J. Evaluating the advective Brewer-Dobson circulation in three reanalyses for the period 1979-2012. *Journal of Geophysical Research (Atmospheres)* **120**, 7534–7554 (2015).

26. Zubov, V., Rozanov, E., Egorova, T., Karol, I. & Schmutz, W. Role of external factors in the evolution of the ozone layer and stratospheric circulation in 21st century. *Atmospheric Chemistry & Physics* **13**, 4697–4706 (2013).

27. Tummon, F. *et al.* Intercomparison of vertically resolved merged satellite ozone data sets: interannual variability and long-term trends. *Atmospheric Chemistry & Physics Discussions* **14**, 25687–25745 (2014).

28. Froidevaux, L. *et al.* Global OZone Chemistry And Related Datasets for the Stratosphere (GOZCARDS): methodology and sample results with a focus on HCl, H_2O, and O_3. *Atmospheric Chemistry & Physics Discussions* **15**, 5849–5957 (2015).

29. McPeters, R. D., Bhartia, P. K., Haffner, D., Labow, G. J. & Flynn, L. The version 8.6 SBUV ozone data record: An overview. *Journal of Geophysical Research (Atmospheres)* **118**, 8032–8039 (2013).

30. Ineson, S. *et al.* Regional climate impacts of a possible future grand solar minimum. *Nature Communications* **6** (2015).

31. Floyd, L. E., Cook, J. W., Herring, L. C. & Crane, P. C. SUSIM'S 11-year observational record of the solar UV irradiance. *Advances in Space Research* **31**, 2111–2120 (2003).

32. Yeo, K. L. *et al.* UV solar irradiance in observations and the NRLSSI and SATIRE-S models. *Journal of Geophysical Research (Space Physics)* **120**, 6055–6070 (2015). `1507.01224`.

33. Lean, J., Rottman, G., Harder, J. & Kopp, G. SORCE Contributions to New Understanding of Global Change and Solar Variability. *Journal of Solar Physics* **230**, 27–53 (2005).

34. Morrill, J. S., Floyd, L. & McMullin, D. Comparison of Solar UV Spectral Irradiance from SUSIM and SORCE. *Solar Physics* **289**, 3641–3661 (2014).

35. Stenke, A. *et al.* The SOCOL version 3.0 chemistry-climate model: description, evaluation, and implications from an advanced transport algorithm. *Geoscientific Model Development* **6**, 1407–1427 (2013).

36. Eyring, V. & Lamarque, J.-F. e. a. Overview of IGAC/SPARC Chemistry-Climate Model Initiative (CCMI) Community Simulations in Support of Upcoming Ozone and Climate Assessments. *SPARC Newsletter* **40**, 48–66 (2013).

37. Dee, D. P. *et al.* The ERA-Interim reanalysis: configuration and performance of the data assimilation system. *Quarterly Journal of the Royal Meteorological Society* **137**, 553–597 (2011).

38. Kuchar, A., Sacha, P., Miksovsky, J. & Pisoft, P. The 11-year solar cycle in current reanalyses: a (non)linear attribution study of the middle atmosphere. *Atmos. Chem. Phys.* **15**, 6879–6895 (2015).

39. Sato, M., Hansen, J. E., McCormick, M. P. & Pollack, J. B. Stratospheric aerosol optical depths, 1850-1990. *Journal of Geophysical Research: Atmospheres* **98**, 22987–22994 (1993). URL `http://dx.doi.org/10.1029/93JD02553`.

40. NCAR. The climate data guide: Multivariate enso index. `https://climatedataguide.ucar.edu/climate-data/multivariate-enso-index` (2013).

41. Efron, B. & Tibshirani, R. J. *An introduction to the bootstrap* (CRC press, 1994).

Data Sources SATIRE-S data was downloaded from `http://www2.mps.mpg.de/projects/sun-climate/data.html`, NRLSSI data from `http://lasp.colorado.edu/lisird/`, and SORCE data from `http://lasp.colorado.edu/home/sorce/`. GOZCARDS ozone data can be accessed at `https://gozcards.jpl.nasa.gov/`, SWOOSH at `http://www.esrl.noaa.gov/csd/groups/csd8/swoosh/`, SBUV-Mod at `http://acd-ext.gsfc.nasa.gov/Data_services/merged/`, and SBUV-Merged at `ftp://ftp.cpc.ncep.noaa.gov/SBUV_CDR/`.

Correspondence Correspondence and requests for materials should be addressed to W.T.B. (email: william.ball@pmodwrc.ch).

Acknowledgements W.T.B. was funded by the SNSF projects 149182 (SILA) and 163206 (SIMA). We thank A. Stenke and A. Coulon for their advice, comments and help with the model nudging. We thank Marty Snow for his comments on SORCE/SOLSTICE. We thank the GOZCARDS, SWOOSH and SBUV teams for their ozone products. E.V.R. was partially supported by the Swiss National Science Foundation under grant agreement CRSII2-147659 (FUPSOL II).

Author Contributions W.T.B. prepared the solar data, performed the model experiments, carried out the linear analysis and interpretation of results. W.T.B and J.D.H wrote the paper. W.T.B, T.S. and E.V.R. designed and set up the model simulations, F.T. provided the ozone datasets and advice on their use, A.V.S. prepared the CCM model nudging and A.K. performed the MLR analysis. J.D.H., E.V.R. and W.S. provided expert advice and discussion on the results.

Competing Interests The authors declare that they have no competing financial interests.

Figure 1 Illustration of photolytic solar cycle ozone response. The solar max-min photolytic ozone response to integrated-UV below 242 nm (left column) produces ozone. Below 320 nm (middle), O_3 photolysis leads to catalytic loss of O_3 if the O does not recombine with O_2. The resultant response (right) is approximately the sum of these [9]. The far larger SORCE changes at ozone destroying wavelengths more than compensates for the larger UV changes at shorter wavelengths, leading to a negative response higher up, while SATIRE-S is positive at all altitudes. Pressure levels are illustrative of Figure 4. Percentages are the relative solar cycle changes.

Figure 2 Solar irradiance and ozone timeseries. (**a**) Daily and smoothed 250–300 nm integrated spectral irradiance for SATIRE-S (blue) and NRLSSI (red, smoothed only) models, and SORCE/SIM observations (black) and extrapolated-SORCE (green; dashed lines bound extrapolation period); the bar represents 1% variability. (**b**) 1.6 hPa ($\sim$43 km) zonal ozone (20°S–20°N averaged) from SWOOSH (black) and constant-Sun simulation (red). (**c**) Residuals from the constant-Sun simulation for SWOOSH (monthly, grey; 24-month running mean, black; 1σ uncertainty, shading), SATIRE-S (blue) and extrapolated-SORCE (green). SWOOSH is bias-shifted by 0.26 ppm to the constant-Sun simulation around 2008. Vertical bars indicate solar maxima/minima (solid/dotted).

Figure 3 Ozone response from multi-linear regression between 1991 and 2012. Solar cycle mean responses and 2σ uncertainties for SWOOSH and GOZCARDS ozone composites (dot-bar) and for SORCE (green line and shading) and SATIRE-S (blue line and shading) simulations. The ozone response is in term of 100 solar flux units of the 10.7 cm radio flux, ∼80% of the solar cycle.

Figure 4 Solar cycle maximum to minimum ozone response from linear fitting. The extracted solar cycle ozone change using Theil-Sen trend analysis (2σ error bars) from the residuals of the constant-Sun simulation (e.g. in Fig 2c) with ozone time series for 1991/07–1996/05 (dashed, circles) and 2002/02–2008/12 (solid, filled circles). SWOOSH (black) and GOZCARDS (orange) are given for both periods, SBUV-Merged (pink) and SBUV-Mod (purple) for the latter period. SATIRE-S (blue) and SORCE (green) shading combines the 2σ errors from both periods with the change between six-month averages at maximum and minimum; NRLSSI is shown for the latter period.

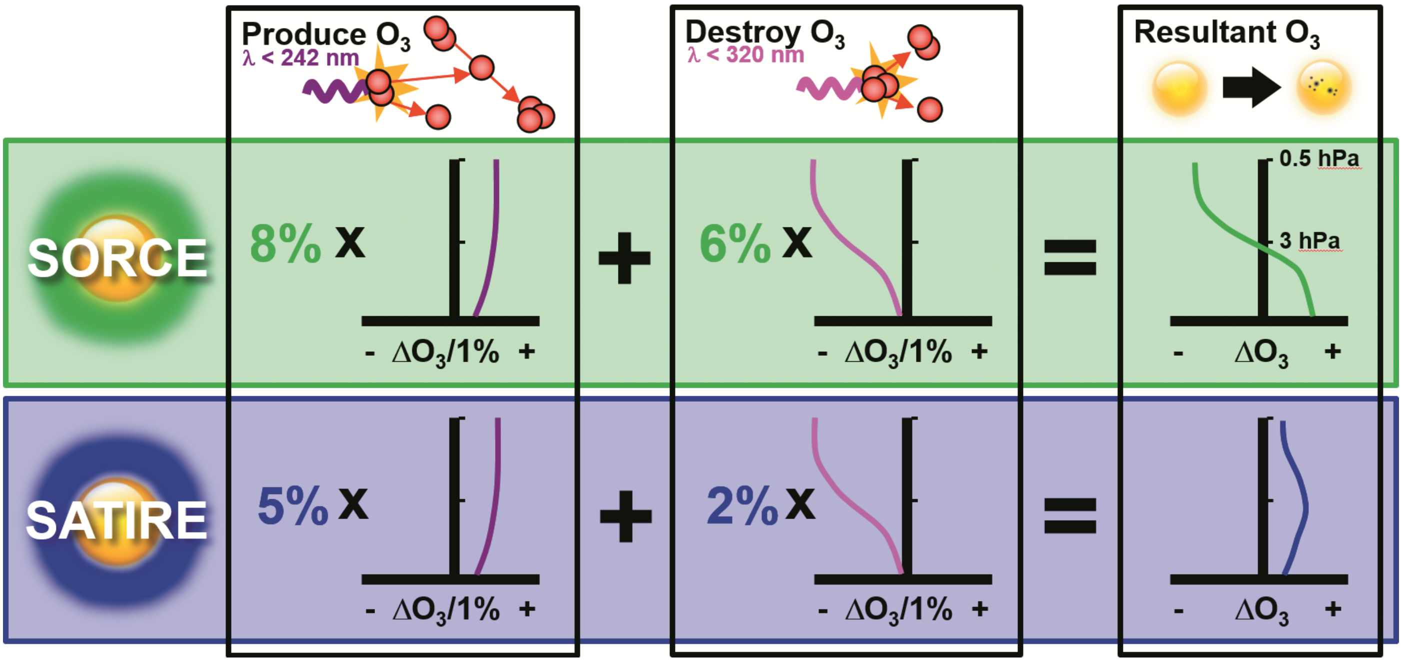
Produce O_3
λ < 242 nm
Destroy O_3
λ < 320 nm
Resultant O_3
SORCE
8% x
- ΔO_3/1% +
+
6% x
- ΔO_3/1% +
=
0.5 hPa
3 hPa
- ΔO_3 +
SATIRE
5% x
- ΔO_3/1% +
+
2% x
- ΔO_3/1% +
=
- ΔO_3 +

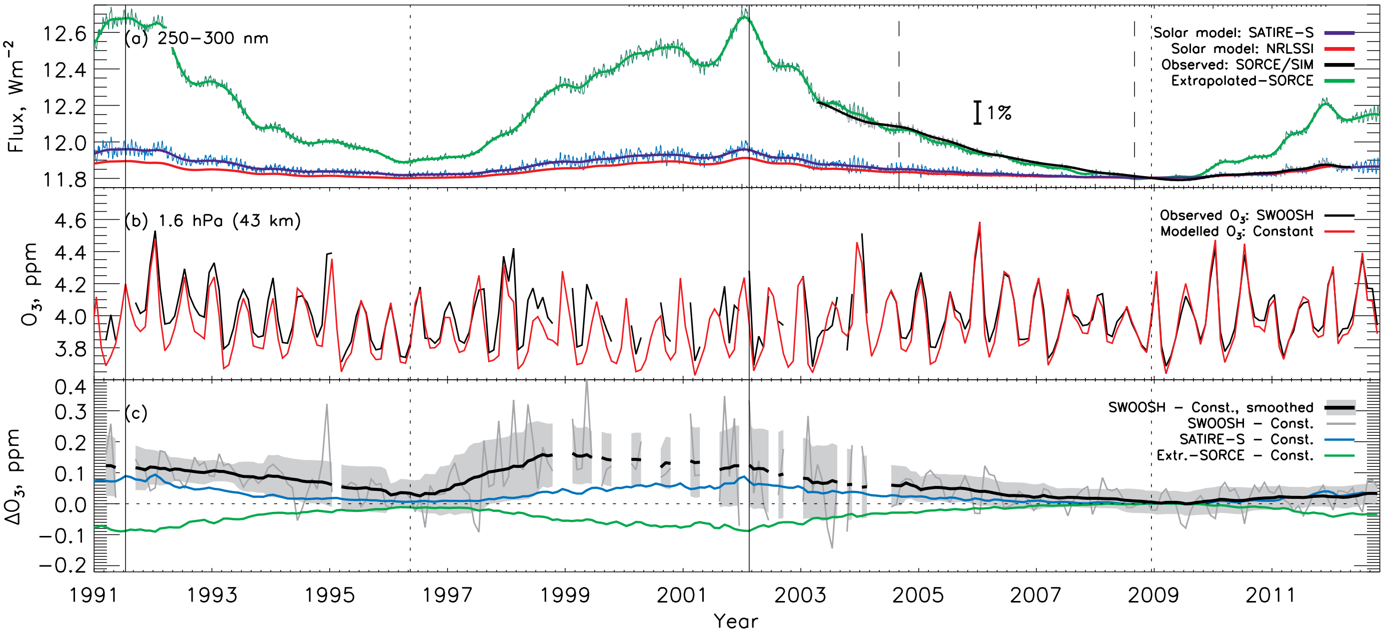
(a) 250−300 nm
Flux, Wm^{-2}
12.6
12.4
12.2
12.0
11.8
1%
Solar model: SATIRE−S
Solar model: NRLSSI
Observed: SORCE/SIM
Extrapolated−SORCE
(b) 1.6 hPa (43 km)
O$_3$, ppm
4.6
4.4
4.2
4.0
3.8
Observed O$_3$: SWOOSH
Modelled O$_3$: Constant
(c)
ΔO$_3$, ppm
0.4
0.3
0.2
0.1
0.0
−0.1
−0.2
SWOOSH − Const., smoothed
SWOOSH − Const.
SATIRE−S − Const.
Extr.−SORCE − Const.
1991
1993
1995
1997
1999
2001
2003
2005
2007
2009
2011
Year

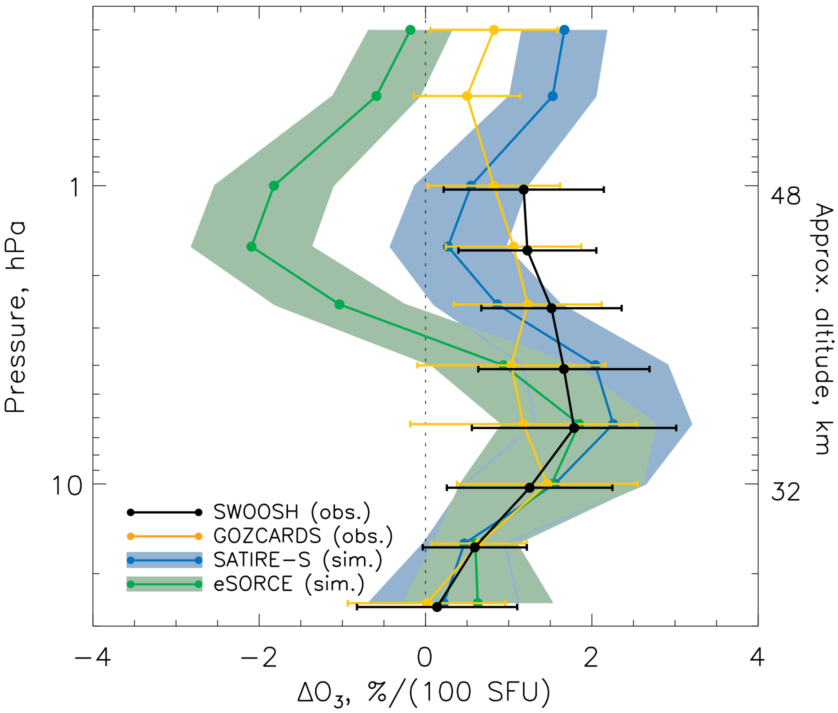
Pressure, hPa
1
10
48
32
Approx. altitude, km
−4
−2
0
2
4
ΔO_3, %/(100 SFU)
SWOOSH (obs.)
GOZCARDS (obs.)
SATIRE−S (sim.)
eSORCE (sim.)

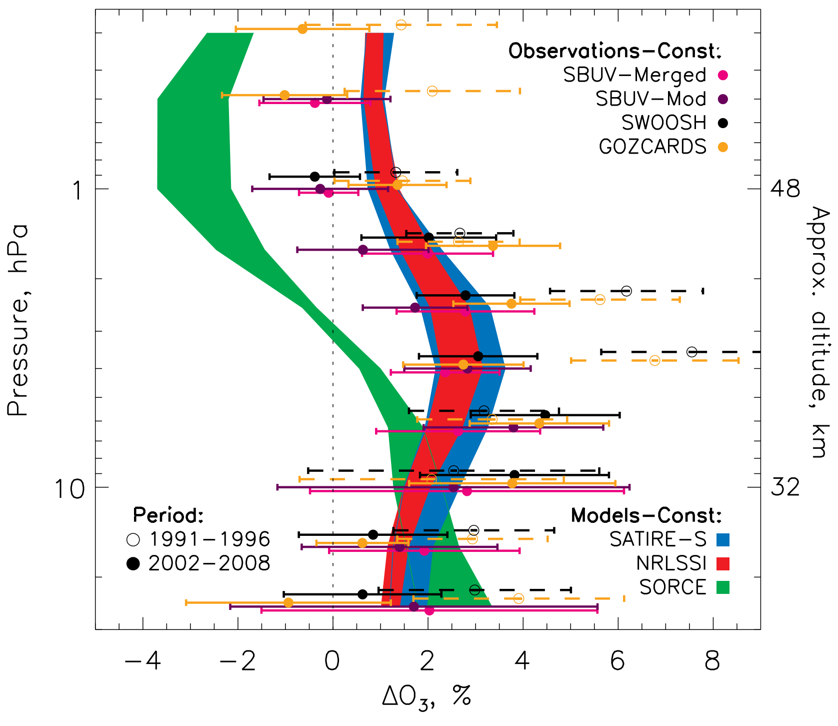
Observations−Const:
SBUV−Merged
SBUV−Mod
SWOOSH
GOZCARDS
Period:
○ 1991−1996
● 2002−2008
Models−Const:
SATIRE−S
NRLSSI
SORCE
Pressure, hPa
1
10
Approx. altitude, km
48
32
−4
−2
0
2
4
6
8
ΔO_3, %